frontiers | Frontiers in Mechanical Engineering

TYPE Original Research
PUBLISHED 01 December 2023
DOI 10.3389/fmech.2023.1325040

OPEN ACCESS

EDITED BY
Vijay Raghunathan,
King Mongkut's University of Technology North Bangkok, Thailand

REVIEWED BY
Jitendra Kumar Katiyar,
SRM Institute of Science and Technology, India
Vinod Ayyappan,
King Mongkut's University of Technology North Bangkok, Thailand

*CORRESPONDENCE
Ranjan Kumar Ghadai,
ranjan.ghadai@manipal.edu
Kanak Kalita,
drkanakkalita@veltech.edu.in

RECEIVED 20 October 2023
ACCEPTED 20 November 2023
PUBLISHED 01 December 2023

CITATION
Ghadai RK, Shanmugasundar G, Cepova L, Das S, Kumar Mahto P and Kalita K (2023), A temperature-based synthesis and characterization study of aluminum-incorporated diamond-like carbon thin films.
Front. Mech. Eng 9:1325040.
doi: 10.3389/fmech.2023.1325040

A temperature-based synthesis and characterization study of aluminum-incorporated diamond-like carbon thin films

Ranjan Kumar Ghadai[1]*, G. Shanmugasundar[2], Lenka Cepova[3], Soham Das[4], Premchand Kumar Mahto[4] and Kanak Kalita[5,6]*

[1]Department of Mechanical and Industrial Engineering, Manipal Institute of Technology, Manipal Academy of Higher Education, Manipal, India, [2]Department of Mechanical Engineering, Sri Sairam Institute of Technology, Chennai, India, [3]Department of Machining, Assembly and Engineering Metrology, Faculty of Mechanical Engineering, VSB-Technical University of Ostrava, Ostrava, Czechia, [4]Department of Mechanical Engineering, Sikkim Manipal Institute of Technology, Sikkim Manipal University, Majhitar, India, [5]Department of Mechanical Engineering, Vel Tech Rangarajan Dr. Sagunthala R&D Institute of Science and Technology, Avadi, India, [6]University Centre for Research and Development, Chandigarh University, Mohali, India

The present work deals with the study of various properties of aluminum (Al)-incorporated diamond-like carbon (DLC) thin films synthesized using the atmospheric pressure chemical vapor deposition (APCVD) technique by varying the deposition temperature (T_d) and keeping the N_2 flow rate constant. Surface morphology analysis, resistance to corrosion, nanohardness (H), and Young's modulus (E) of the coatings were carried out using atomic force microscopy (AFM), corrosion test, scanning electron microscopy (SEM), and nanoindentation test, respectively. SEM results showed a smoother surface morphology of the coatings grown at different process temperatures. With an increase in process temperature, the coating roughness (Ra) lies in the range of 20–36 µm. The corrosion resistance of the coating was found to be reduced with a consecutive increase in the deposition temperature from 800°C to 880°C. However, above 880°C, the resistance increases further, and it may be due to the presence of more Al weight percentage in the coating. The nanoindentation result revealed that H and E of the coating increase with an increase in the CVD process temperature. The elastic–plastic property indicated by H/E and H^3/E^2, which are also indicators of the wear properties of the coating, were studied using the nanoindentation technique. The residual stresses (σ) calculated using Stoney's equation revealed a reduction in residual stress with an increase in the process temperature.

KEYWORDS

aluminum-incorporated diamond-like carbon, nanoindentation, residual stress, thin film, coatings

1 Introduction

Coatings play a crucial role in enhancing the performance and durability of various materials and surfaces. They offer a protective barrier against corrosion, wear, and other forms of degradation while also providing desirable properties, such as high hardness and low friction. Diamond-like carbon (DLC) thin films are a type of polycrystalline coating, which possess a very dense carbon crystalline network. These coatings have become popular due to their inherent properties such as higher hardness (H), Young's modulus (E),

corrosion resistance and wear resistance (WR), and a lower coefficient of friction (COF) (Singh et al., 2005). This desirable combination of properties has led to a wide range of applications in various fields, like automotive, aerospace, electronics, and biomedical (Bhushan and Ko, 2003). However, the inherent brittleness and low electrical conductivity of DLC films have limited their use in many critical applications. To address these limitations, several researchers have explored the incorporation of metals such as aluminum into DLC films. The resulting aluminum-incorporated DLC (Al-DLC) thin films have been shown to have improved properties and performance.

In recent years, metal-incorporated DLC coatings have been extensively studied by various research groups due to their higher chemical inertness, low residual stress (σ), and excellent mechanical and tribological properties (Ghadai et al., 2018). Addition of aluminum has been shown to increase the toughness, electrical conductivity, and thermal stability of DLC films while maintaining their advantageous properties, such as high hardness and low friction (Voevodin et al., 1999). Moreover, addition of aluminum can also modify the optical properties of DLC films, enabling tailored applications in the field of optics (Erdemir and Donnet, 2006). It has been reported that Al-doped carbon-based thin films resulted in a reduction of internal stress with improved toughness of DLC thin films (Zhang et al., 2002). Tay et al. (2001) reported a reduction in σ of Al-doped DLC thin films due to reduced sp^3 hybridization within the films. Guo et al. (2017) synthesized Al/Ti-doped DLC coatings using a unique hybrid ion-beam system and observed a minimum σ of 1.28 ± 0.1 GPa and maximum H of 20 GPa. Huang et al. (2023a) analyzed the tetrahedral carbon aluminum film using a large-scale atomic parallel simulator and observed that Al plays a significant role in the properties of the developed coating. Wongpanya et al. (2022) synthesized a DLC coating with Al and N doping over AISI 4140 steel using the filtered cathodic vacuum-arc technique and observed that the corrosion resistance and adhesion performance of the developed coating significantly enhanced compared to those of DLC coating.

Both physical vapor deposition (PVD) and chemical vapor deposition (CVD) methods have been used for the synthesis of Al-DLC thin films. Magnetron sputtering is a popular PVD technique used for the deposition of Al-DLC thin films due to its advantages in terms of high deposition rates, good film adhesion, and scalability (Kong et al., 2018). In magnetron sputtering, the target material is bombarded with high-energy ions, resulting in the sputtering of carbon and aluminum atoms, which are then deposited onto a substrate to form the Al-DLC film. The deposition temperature is controlled by adjusting the power applied to the target and substrate heating (Bouabibsa et al., 2018). Pulsed-laser deposition (PLD) is another popular PVD technique that has been employed for the synthesis of Al-DLC thin films (Ni et al., 2006). In the PLD method, a high-energy laser pulse ablates the target material, which generates a plasma plume that is deposited onto a substrate to form the film. PLD enables the precise control of the film composition and deposition temperature by adjusting the laser energy, pulse frequency, and substrate temperature. PLD produces highly crystalline and uniform films, which makes it a suitable method for synthesizing tailor-made Al-DLC thin films (Ding et al., 2021).

Plasma-enhanced chemical vapor deposition (PECVD) is a popular CVD technique used for depositing Al-DLC films since it produces high-quality films at relatively low temperatures (Huang et al., 2023b). In PECVD, a gaseous mixture of hydrocarbon and aluminum precursors in a reaction chamber is subjected to electrical discharges. This generates plasma, which causes film deposition onto the substrate. The deposition in PECVD can be controlled by adjusting the power input, precursor flow rates, and substrate heating (Huang et al., 2023b). Similarly, hot-filament chemical vapor deposition (HFCVD) is another CVD method used for the synthesis of Al-DLC films. In HFCVD, a hot filament is used to thermally decompose hydrocarbon and aluminum precursors in a gaseous mixture, which leads to the deposition of carbon and aluminum atoms onto the heated substrate (Pang et al., 2010). In HFCVD, the film properties can be the fine-tuned by adjusting the filament temperature and substrate heating.

Thus, it is noted that each technique offers certain advantages and drawbacks over the other. PVD techniques like magnetron sputtering and PLD generally have higher deposition rates, better film adhesion, and greater scalability (Ding et al., 2022). However, PVD techniques may suffer from issues related to film uniformity and stoichiometry control. On the other hand, CVD methods like PECVD and HFCVD can produce high-quality films at lower temperatures, making them more preferable for temperature-sensitive substrates (Huang et al., 2023b). CVD techniques also offer better control over film composition and uniformity but generally require longer deposition times (Pang et al., 2010).

Additionally, the literature review reveals that few researchers deposited the Al-DLC coating using physical vapor deposition techniques and obtained a reduction in the σ value. However, PVD techniques exhibit poor step coverage in the case of applications related to silicon devices because of the increased aspect ratio of contact through trenches. This limitation is diminished in the case of chemical vapor deposition techniques, and the possibility of surface uniformity with CVD techniques is finer than that in PVD techniques (Irudayaraj et al., 2007).

In the present work, the synthesis of the Al-DLC coating has been carried out using the atmospheric pressure chemical vapor deposition (APCVD) technique. The objective of this study is to fill this knowledge gap by systematically investigating the influence of deposition temperature on the surface morphology, resistance to corrosion, nanohardness (H), and Young's modulus (E). The elastic–plastic properties of the coatings, as indicated by the H/E and H^3/E^2 ratios, which are considered important indicators of wear properties, were also investigated. The residual stresses (σ) in the film were also calculated using Stoney's equation, and their dependence on the deposition temperature was also investigated.

This paper is organized as follows: Section 1 presents a brief introduction to the need for Al incorporation into DLC films and reviews a few relevant literature works. Section 2 describes the experimental methods used in this study. The process of synthesis of Al-DLC films by the APCVD technique and the characterization techniques employed to investigate the surface morphology, resistance to corrosion, nanohardness, and Young's modulus of the coatings are discussed in Section 2. Section 3 presents and discusses the results obtained from the analysis of the films, including the effects of the deposition temperature on the coating roughness, corrosion resistance, nanoindentation

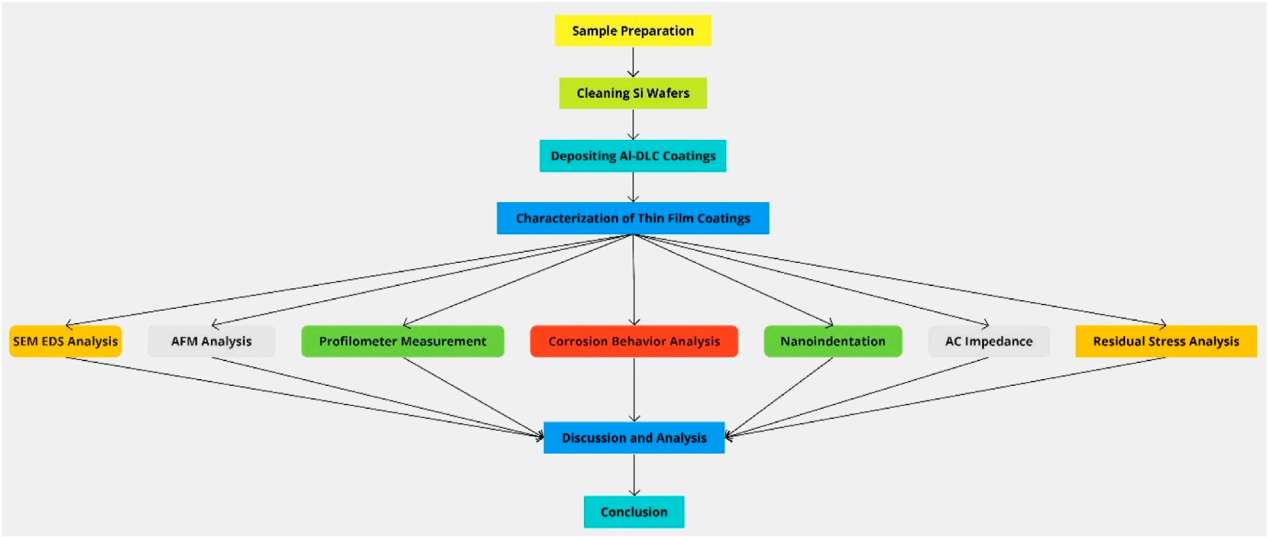

FIGURE 1
Flowchart depicting the methodology for the synthesis and characterization of Al-DLC coatings.

TABLE 1 Details of the deposition parameter and film thickness of Al-DLC thin films.

Sl. no.	C_2H_2 flow rate (sccm)	N_2 flow rate (sccm)	Temperature (°C)	Film thickness (μm)
1	7	20	800	3.88 ± 0.19
2	7	20	840	3.12 ± 0.45
3	7	20	880	2.96 ± 0.36
4	7	20	920	2.88 ± 0.16

properties, and residual stresses. Section 4 presents a general discussion on the effect of the deposition temperature on AL-DLCs. Finally, Section 5 summarizes the main findings and conclusions of the study.

2 Experimental details

The methodology followed in this work is shown in Figure 1.

2.1 Sample preparation

DLC coatings were deposited over Si (100) wafers. Before the synthesis of thin films, Si wafers were cleaned using the Radio Corporation of America (RCA) cleaning process, whose detailed explanation can be found in some other literature (Das et al., 2022). The substrates were kept in an APCVD chamber by placing them over an alumina ceramic boat. The synthesis of Al-DLCs was carried out using pure Al powder (99.9%). The Al-DLC samples were prepared by varying T_d from 800°C to 920°C and keeping the acetylene (C_2H_2) and nitrogen (N_2) flow rates constant. The deposition time was fixed at 1 hour after reaching the required deposition temperature. The heating rate was set at 5°C/min, and the cooling rate was set at 3°C/ min. The base pressure was set at 5×10^{-6} Torr, and the process pressure was maintained at 500 mTorr. Table 1 indicates the details of the gas flow rate, film thickness, and process temperature used for deposition.

2.2 Thin-film coating characterization

The morphology and elemental composition of the coatings were analyzed using an SEM EVO MA18 instrument with an Oxford EDS (X-act) magnification range of ×1 to ×100,000. The AFM technique was used to evaluate the coating roughness (Ra) using Innova SPM (scanner 100 μm). The thin-film coating thickness was evaluated using a Dektak profilometer (Dektak 300 V). The corrosion behavior of DLC films was studied using CHI Software by plotting the curve between E_{corr} and I_{corr}. The samples were dipped in 1 M H_2SO_4 solution prepared by mixing distilled water and chemical-grade reagents. The corrosion test was conducted at room temperature under open-air conditions, with a scan rate in the range of 0.1–0.5 V/s; Al-DLC samples were used as a working electrode, and Ag/AgCl and platinum acted as reference and counter electrodes, respectively. The nanoindentation technique was used to evaluate H and E of Al-DLC films using an NHTX 55-0019 nanohardness tester equipped with a Berkovich diamond

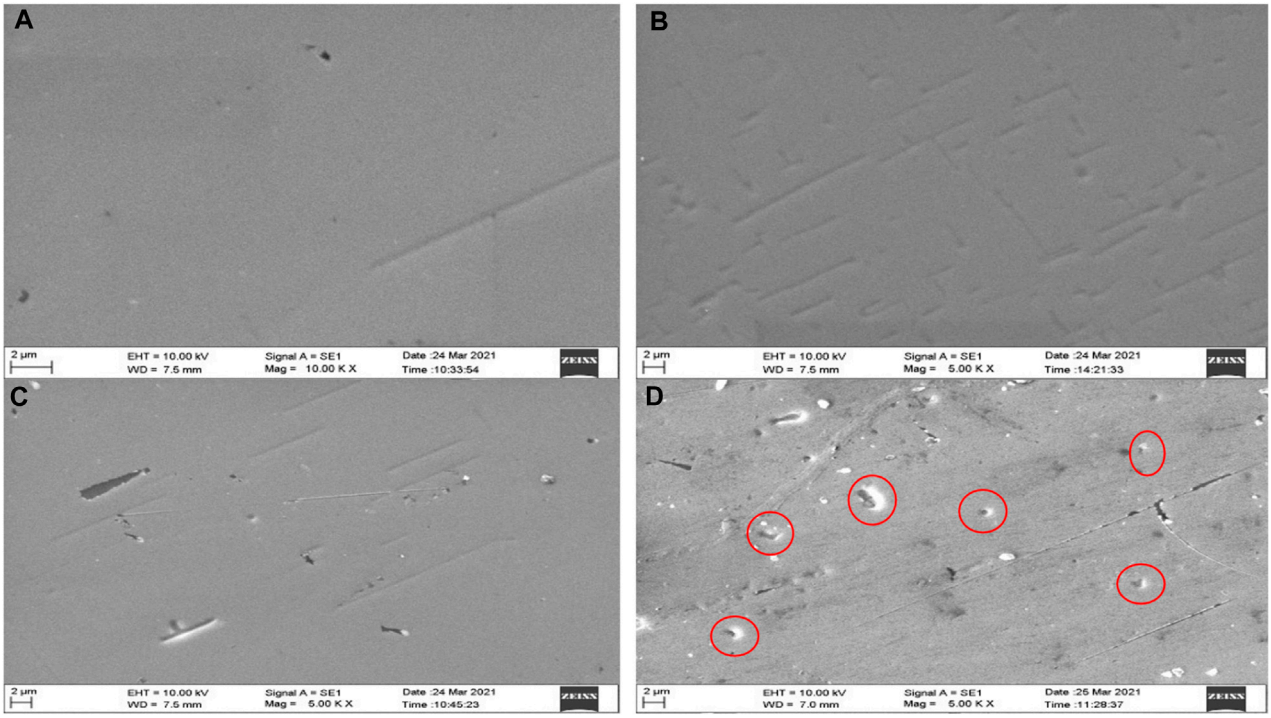

FIGURE 2
SEM micrographs of AL-DLC thin films prepared at **(A)** 800°C, **(B)** 840°C, **(C)** 880°C, and **(D)** 920°C.

indenting tip (B-I 93; radius of curvature 20 μm). The H value of the coatings was calculated at four different points of samples with a fixed load of 18 mN.

3 Characterization results

3.1 Thickness and morphological analysis

The coating thickness of Al-DLC with respect to various deposition temperatures is listed in Table 1. From the table, it is observed that the coating thickness decreases with respect to the deposition temperature. The deposition rate depends on many parameters, like the deposition temperature, gas flow rate, deposition time, deposition pressure, and substrate position. With the increase in the deposition temperature, the particles in the deposition layer gradually become larger, leading to the gradual increase in thickness. The increase in the temperature leads to an increase in the growth rate of the nuclei, and the particles begin to fuse with each other to form cellular particles. Therefore, the porosity of the coating decreases, while its density increases (Bi et al., 2022). Furthermore, at a high temperature, the movement of gas molecules inside the chamber will be higher, which results in a rough surface and film thickness. The SEM images of the Al-DLC samples prepared at different T_d are shown in Figure 2. The SEM micrographs show a smooth texture for all the samples grown at different T_d. However, no distinct grain pattern is evident from the SEM images. Notably, the coating prepared at the temperature of 920°C exhibits distinct, white-colored spots over its surface, and they have been marked by red circles. These spots may be attributed to white agglomerated particles that could have been deposited at the time of deposition due to partial melting and evaporation of the powder particles. The coatings are observed with negligible pores and inclusions. Furthermore, the surface of the coatings appears smoother than those deposited at 920°C. In previous research works, it is reported that the morphology of the coatings greatly depends on atom diffusion, deposition, and etching effect (Liang et al., 2007). The proper estimation of the grain size or particle size of the coatings is further characterized by AFM. The composition of various elements of Al-DLC coatings prepared under various process temperatures is listed in Table 2. The results of EDS reveal that with an increase in T_d (800°C to 880°C), the atomic% of C increases and that of Al decreases. However, for the deposition temperature of 920°C, the atomic% of C is the lowest and that of Al is the highest.

TABLE 2 Composition of various elements of Al-DLC thin films using EDS.

Sample no.	% of carbon	% of Al	% of N_2
Al-DLC 800°C	90.46	9.12	0.42
Al-DLC 840°C	91.26	8.18	0.56
Al-DLC 880°C	91.61	8.03	0.36
Al-DLC 920°C	90.31	9.16	0.53

The EDS results, as shown in Figure 3, reveal that the concentration of Al in the Al-DLC film decreases with an increase in T_d of up to 880°C. However, above 880°C, Al concentration increases further. Similarly, nanoindentation plots

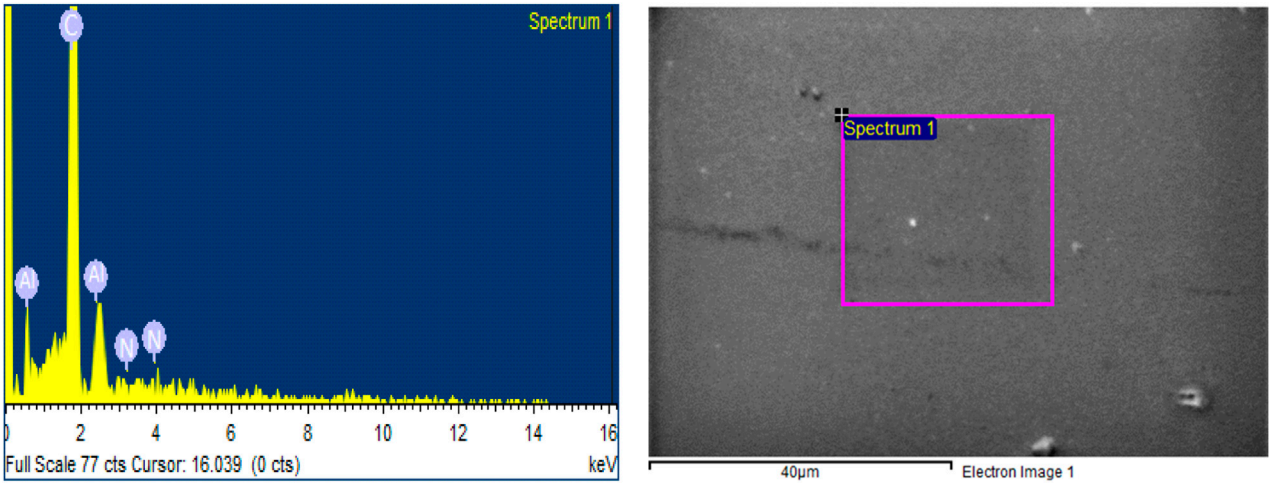

FIGURE 3
EDS analysis of the Al-DLC coating prepared at 800°C using APCVD.

reveal that the H of DLC thin films decreases with the increase in T_d. It has been reported in previous studies that the concentration of the film decreases with the increase in H (Liu et al., 2005). The σ value of Al-DLC thin films for various T_d is shown in Figure 8. In the present case, the σ value of the film is more for the DLC film deposited at 800°C, and the σ value decreases with an increase in the deposition temperature. The decrease in σ at higher temperatures may be due to the heat treatment phenomena. Furthermore, at higher temperatures, at.% of Al in the film increases, which tends to decrease the σ value (Zhou et al., 2019).

3.2 Surface roughness using AFM

The surface morphology of Al-DLC coatings characterized by the AFM technique is shown in Figure 4. The Al-DLC thin films prepared at 800°C, 840°C, 880°C, and 920°C showed the maximum particle sizes of 29.0, 10.3, 29.4, and 18.3 nm, respectively. The AFM images also revealed globular-shaped grains of C and Al atoms unevenly distributed throughout the surface of the coating. The Al-DLC thin films prepared at 840°C, 880°C, and 920°C process temperatures showed large and sharp pyramidal-shaped grains of Al and C atoms all over the surface. Among all the Al-DLC thin films prepared, the coating synthesized at 880°C showed the maximum particle distribution all over the surface. The maximum surface roughness (Ra) of the coatings prepared at different process temperatures was 8.3, 10.28, 12.23, and 7.29 nm, respectively. Pu et al. (2015) reported that the Ra of sputtered Al-DLC thin films was 0.154 and 2.148 nm for the negative bias of 0 and −500 V, respectively. In the present study, a higher value of Ra of the coatings was observed, which may be due to the higher randomness of the gaseous and powder particles inside the CVD chamber, which may have arisen due to a higher N_2 flow rate at a high CVD temperature (Pu et al., 2015). In addition to this, the higher Ra of the coatings could be due to the increasing Sp^2-bonded carbon sites.

3.3 Corrosion behavior of Al-DLC coatings

Figure 5 shows the polarization curve of different Al-DLC thin films through the Tafel plot using diluted water (50 mL) and KCl powder (1.5 g). The polarization curve indicates the corrosion potential (E_{corr}) and corrosion current density (I_{corr}) for various electrodes. E_{corr} and I_{corr} for Al-DLC 800°C, Al-DLC 840°C, Al-DLC 880°C, and Al-DLC 920°C coatings synthesized via APCVD were found to be −0.461 V and −7.26 A/cm^2, −0.6611 V and −6.804 A/cm^2, −0.747 V and −7.238 A/cm^2, and −0.673 V and −6.501 A/cm^2, respectively. The corrosion resistivity of all samples is almost the same, but the curve for Al-DLC films prepared at 800°C is on the rightmost side amongst all others, as shown in Figure 5, which shows the highest corrosion resistivity (Matei et al., 2015). This also means that the Al-DLC nanocomposite material synthesized at lower temperatures is likely to have better corrosion resistivity.

3.4 AC impedance

The kinetic information and the interfacial properties of electrode materials were extracted using the EIS method—a non-destructive and easy method suitable for all coatings (Das et al., 2022). A Nyquist plot was constructed, which presents a plot of real impedance Z′ vs. negative imaginary impedance Z”. Figure 6 shows the Nyquist plots of all Al-DLC coatings prepared at different temperatures ranging from 800°C to 920°C. The semi-circular curves shown in the Nyquist plot indicate the charge transfer resistance (RCT) within the material, whereas the initial semi-circular plot indicates the magnitude of RCT. It provides insights into factors, such as capacitance, charge transfer resistance, and diffusion processes, aiding in the assessment of the Al-DLC coating's corrosion resistance. Figure 6 shows that the Al-DLC thin film deposited at 800°C, observed with a well-defined initial semi-circle, indicated the actively controlled charge transfer process. The smaller semi-circle of the AL-DLC coating prepared at 880°C shows that the

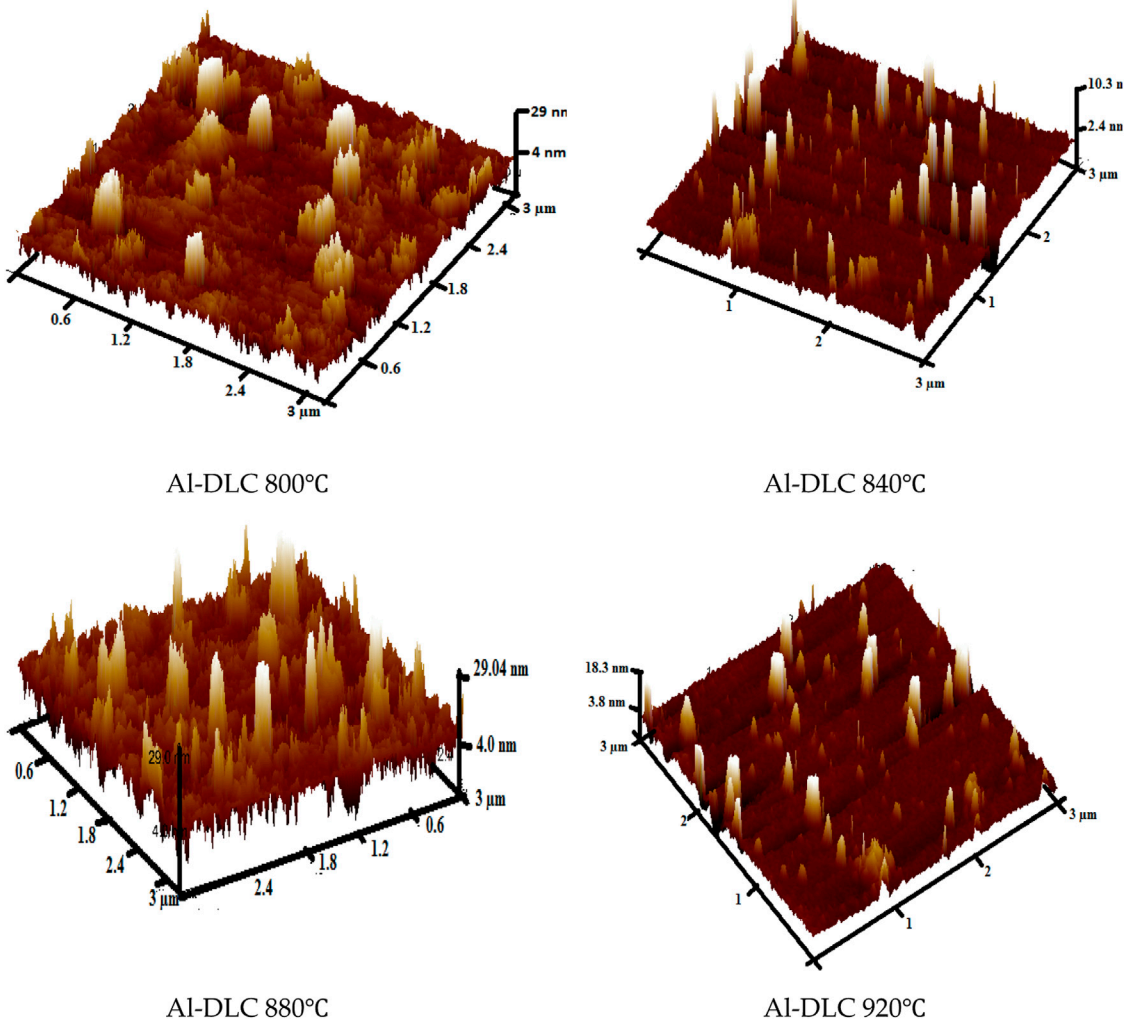

FIGURE 4
Particle size estimation of Al-DLC thin films characterized by AFM.

charge transport is lesser than the other two coatings (Matei et al., 2015). A reduction in RCT is observed due to the enhanced super-capacitive properties, which could be the result of a synergistic effect between Al-DLC 880°C and AL-DLC 800°C coatings.

3.5 Mechanical properties by nanoindentation

The load–displacement curve of Al-DLC coatings prepared at different T_d and constant C_2H_2 and N_2 flow rates is shown in Figure 7. The thin films were subjected to a fixed maximum indentation load of 17 mN. The nanoindentation depth of Al-DLC coatings synthesized at varying temperatures is listed in Table 3. As T_d increases, the maximum indentation depth of Al-DLC thin films increases, which indicates the decrease in the H value. This decrease in H with the increasing process temperature could be due to lesser Al incorporation (in at. wt%) as represented in Table 1. Previous research reports reported that the higher the coating hardness, the smaller the depth of penetration of the nanoindenter, i.e., $H \propto 1/h_{max}$ (Kong and Fu, 2015). The nanoindentation curve of Al-DLC thin films showed pop-out phenomena that could be due to slower loading/unloading rates (Domnich et al., 2000). The maximum H and E of the Al-DLC coating prepared at different temperatures are shown in Table 4. The maximum H and E in the present study are 22.5 ± 1.36 GPa and 212.70 ± 16.89 GPa, respectively. Dai et al. (Robertson, 2002) reported that a reduction in H, E, and the internal stress of the sputtering-coated Al-DLC is observed from 25 GPa to 10 GPa, 150 GPa to 50 GPa, and 1.5 GPa to 0.5 GPa, respectively, with an increasing Al concentration from 0.68% to 17.7%. In general, the H value of the DLC thin film is reported as 35 GPa–42 GPa (Dai and Wang, 2011). The H value of DLC thin films depends on the sp^3 bond fraction.

The plasticity index (η_p), plastic deformation resistance (H^3/E^2), and elasticity index (η_i) of Al-DLC thin films are listed in Table 4. The η_p value of Al-DLC coatings is evaluated using the following relation:

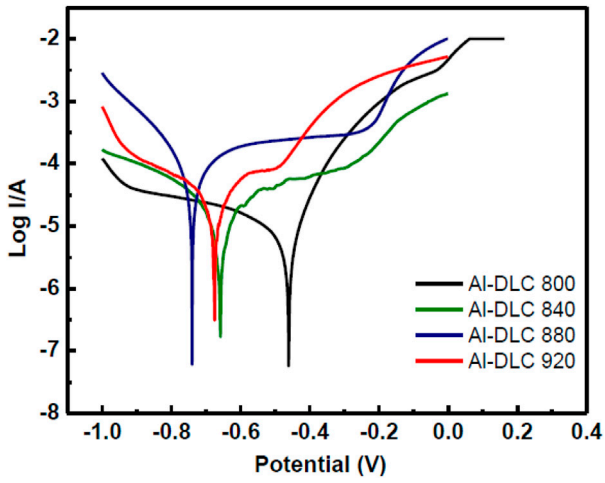

FIGURE 5
Tafel plot of Al-DLC coatings deposited at 800°C, 840°C, 880°C, and 920°C.

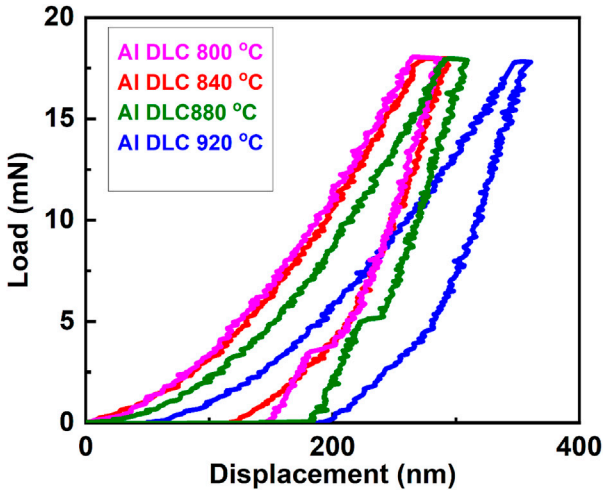

FIGURE 7
Load (mN) vs. displacement (nm) curve of Al-DLC coatings.

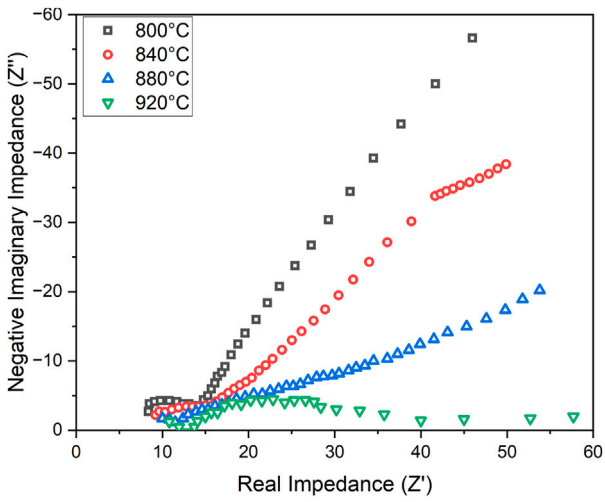

FIGURE 6
Nyquist plots of Al-DLC coatings.

$$\eta_p = \frac{A_1}{A_1 + A_2}. \quad (1)$$

Here, A_1 is the area between the loading and unloading curves and $(A_1 + A_2)$ is the total area during plastic loading. The η_i value of the coatings is calculated using the following equation (Patel et al., 2015):

$$\eta_i = 1 - \eta_p. \quad (2)$$

The plasticity index measures the coating toughness, and plastic deformation resistance (H^3/E^2) is an indicator of the creep resistance of the coating at the point of application of the load (Deng et al., 2014). With the increase in the process temperature, the η_p and η_i values of the coatings prepared at 800°C, 840°C, 880°C, and 920°C were found to be very close to each other, indicating that there is the least effect of the process temperature on the ductility of Al-DLC thin films. The close values of η_i and η_p obtained in the case of Al-DLC coatings prepared at various process temperatures showed a similar nature of the coating plastic deformation and energy dissipation in the indentation region, which may have a considerable effect on H and E of the coating (Yang, 2016). Therefore, the results obtained from Table 4 also conclude that the deposited coatings possessed almost similar toughness.

TABLE 3 Maximum indentation depth of Al-DLC coatings.

Coating	Indentation depth (nm)
Al-DLC 800°C	265.24
Al-DLC 840°C	294.21
Al-DLC 880°C	294.75
Al-DLC 920°C	353.56

3.6 Residual stress analysis

The detachment of films from the parent body leads to higher residual stress (σ) values in DLC thin films, which further causes a restriction to their diverse applications (Peng and Clyne, 1998). Although various attempts have been made to reduce σ in DLC coatings, it remains a complex task to accomplish. However, there are different methods to calculate the σ value in DLC films, but Stoney's equation is the most convenient method to calculate the σ value of the films. The σ value is calculated using Stoney's equation as follows:

$$\sigma = \frac{E_S}{6(1-\upsilon_s)} \times \frac{t_s^2}{t_f}\left(\frac{1}{R_2} - \frac{1}{R_1}\right), \quad (3)$$

where t_s is the substrate thickness, t_f is the film thickness, R_2 is the curvature of the film, R_1 is the substrate curvature before deposition,

TABLE 4 *H* and *E* values of Al-DLC coatings.

Sl. no.	Coating	*H* (GPa)	*E* (GPa)	Plasticity index (η_p)	Elasticity index (η_i)	H^3/E^2
1	Al-DLC 800°C	22.5 ± 1.36	212.70 ± 16.89	0.56	0.438	0.25
2	Al-DLC 840°C	21.65 ± 1.88	205.52 ± 14.33	0.538	0.46	0.24
3	Al-DLC 880°C	16.57 ± 2.12	170.66 ± 12.81	0.56	0.43	0.15
4	Al-DLC 920°C	12.39 ± 1.39	122.74 ± 21.63	0.55	0.448	0.12

υ_s is the Poisson's ratio, and E_S is the Young's modulus of the substrate. The E_S and υ_s for the Si (100) substrate are 127 GPa and 0.27, respectively (Ardigo et al., 2014).

4 Discussion

Thus, this study concludes that the deposition temperature has a significant impact on the morphology and structure of Al-DLC thin films. At lower deposition temperatures, Al-DLC films generally exhibit a more amorphous structure, which is associated with a random arrangement of carbon atoms and a mixture of sp^2- and sp^3-hybridized bonds (Bouabibsa et al., 2018). In contrast, as the deposition temperature increases, the film structure becomes more crystalline, with a higher degree of ordering and an increased fraction of sp^2 bonds (Ghadai et al., 2021). Such a structural transition affects the mechanical, optical, and electrical properties of the films.

It has been reported in the literature that the deposition temperature also influences the grain size and surface roughness of Al-DLC films. As the deposition temperature increases, the grain size generally increases due to the enhanced atomic mobility, which leads to the growth of large crystalline domains (Zhou et al., 2019). The increase in the grain size often results in reduced film hardness and increased surface roughness. However, the exact relationship between deposition temperature, grain size, and surface roughness depend on the synthesis method and experimental conditions. This is why it is important to optimize these parameters for the desired film properties.

From the results of the experiments in the previous section, it is noted that the mechanical properties of Al-DLC films, such as hardness and elastic modulus, are strongly influenced by the deposition temperature. Higher deposition temperatures can lead to increased grain sizes and a more crystalline structure, which results in reduced film hardness (Kong et al., 2018). The DLC coating is basically a mixture of Sp^2 and Sp^3 bonds. The mechanical properties of the coating significantly affect the amount of Sp^2 and Sp^3 bonds present within the coating. The elastic modulus may also decrease with the increasing deposition temperature due to the transition from a more sp^3-rich amorphous structure to a more sp^2-rich crystalline structure (Ghadai et al., 2021). Therefore, it is imperative to control the deposition temperature and optimize it to achieve the desired mechanical properties for specific applications. The residual stress with respect to the deposition temperature is shown in Figure 8. By increasing the deposition temperatures, the residual stress of the coating decreases, which may be due to the heat treatment phenomena.

Deposition temperature also plays a crucial role in determining the chemical composition of Al-DLC films, particularly the aluminum content and its distribution over the film. Because of enhanced surface mobility and diffusion of aluminum atoms, high deposition temperatures can lead to an increase in aluminum incorporation in the film (Ni et al., 2006). However, excessive aluminum content may also result in the formation of aluminum carbide phases, which can negatively impact the film's mechanical and tribological properties (Voevodin et al., 1999). Therefore, careful control of the deposition temperature is needed to achieve the desired aluminum content and distribution in Al-DLC films. This further highlights the need for a carefully crafted design of experiments and optimization for obtaining the best DLC thin films. Due to its high hardness and low residual stress, the developed coating can be used in various automotive engine components, such as piston, piston ring camshaft, valve stem and head, and rocker arm (Voevodin et al., 1999; Zhang et al., 2002; Erdemir and Donnet, 2006; Ghadai et al., 2018). This type of coating can also be used for the development of a biological implant (Tay et al., 2001).

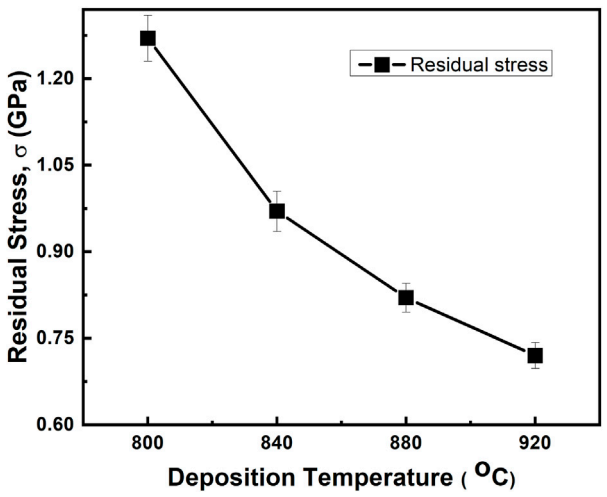

FIGURE 8
Residual stress of Al-DLC thin films at various deposition temperatures.

5 Conclusion

In the present research, Al-DLC coatings were synthesized using the APCVD technique by varying T_d. The AFM images also revealed that the maximum Ra of the coatings prepared at different process temperatures is 8.3, 10.28, 12.23, and 7.29 nm, respectively. The

nanoindentation results revealed that the *H* and *E* of DLC thin films decrease with an increase in the deposition temperature, which is due to the release of internal stress with respect to temperatures. The residual stress of the film decreases with any increase in the deposition temperature. The corrosion results confirmed that the Al-DLC nanocomposite material synthesized at lower temperatures is likely to have better corrosion resistivity; by carefully controlling the deposition temperature, it is possible to tailor the properties of Al-DLC films for specific applications. Further research is warranted to fully understand the complex relationships between deposition temperature, synthesis method, and film properties. Moreover, the need for using optimization to tailor thin-film coatings cannot be overstated. In the future, this study will be extended in this direction by incorporating an appropriate design of experiments and an optimization procedure to achieve enhanced properties for specific applications.

Data availability statement

The raw data supporting the conclusion of this article will be made available by the authors, without undue reservation.

Author contributions

RG: conceptualization, data curation, formal analysis, investigation, methodology, and writing–original draft. GS: conceptualization, methodology, and writing–original draft. LC: conceptualization, methodology, resources, and writing–review and editing. SD: data curation, formal analysis, investigation, and writing–original draft. PK: data curation, formal analysis, investigation, and writing–original draft. KK: resources, visualization, and writing–review and editing.

Funding

The authors declare that no financial support was received for the research, authorship, and/or publication of this article.

Conflict of interest

The authors declare that the research was conducted in the absence of any commercial or financial relationships that could be construed as a potential conflict of interest.

The author(s) declared that they were an editorial board member of Frontiers, at the time of submission. This had no impact on the peer review process and the final decision.

Publisher's note

References

Ardigo, M. R., Ahmed, M., and Besnard, A. (2014). Stoney formula: Investigation of curvature measurements by optical profilometer. *Adv. Mat. Res.* 996, 361–366. doi:10.4028/www.scientific.net/amr.996.361

Bhushan, B., and Ko, P. L. (2003). Introduction to tribology. *Appl. Mech. Rev.* 56 (1), B6–B7. doi:10.1115/1.1523360

Bi, M., Zhu, J., Luo, Y., Cai, H., Li, X., Wang, X., et al. (2022). Effect of deposition temperature on the surface, structural, and mechanical properties of HfO2 using chemical vapor deposition (CVD). *Coatings* 12, 1731. doi:10.3390/coatings12111731

Bouabibsa, I., Lamri, S., and Sanchette, F. (2018). Structure, mechanical and tribological properties of Me-doped diamond-like carbon (DLC)(Me= Al, Ti, or Nb) hydrogenated amorphous carbon coatings. *Coatings* 8, 370. doi:10.3390/coatings8100370

Dai, W., and Wang, A. (2011). Deposition and properties of Al-containing diamond-like carbon films by a hybrid ion beam sources. *J. Alloys Compd.* 509, 4626–4631. doi:10.1016/j.jallcom.2011.01.132

Das, S., Guha, S., Ghadai, R., Sharma, A., and Chatterjee, S. (2022). Morphological, mechanical property analysis and comparative study over structural properties of CVD TiN film grown under different substrate temperature in nitrogen gas atmosphere. *Silicon* 14, 183–199. doi:10.1007/s12633-020-00807-5

Deng, B., Pei, J. F., and Tao, Y. (2014). Microstructure, mechanical and tribological properties of the TiAlN coatings after Nb and C dual ion implantation. *Mat. Sci. For.* 789, 455–460. doi:10.4028/www.scientific.net/msf.789.455

Ding, J. C., Chen, M., Mei, H., Jeong, S., Zheng, J., Yang, Y., et al. (2022). Microstructure, mechanical, and wettability properties of Al-doped diamond-like films deposited using a hybrid deposition technique: bias voltage effects. *Diam. Relat. Mater.* 123, 108861. doi:10.1016/j.diamond.2022.108861

Ding, J. C., Mei, H., Zheng, J., Wang, Q. M., Kang, M. C., Zhang, T. F., et al. (2021). Microstructure and wettability of novel Al-containing diamond-like carbon films deposited by a hybrid sputtering system. *J. Alloys Compd.* 868, 159130. doi:10.1016/j.jallcom.2021.159130

Domnich, V., Gogotsi, Y., and Dub, S. (2000). Effect of phase transformations on the shape of the unloading curve in the nanoindentation of silicon. *Appl. Phys. Lett.* 76, 2214–2216. doi:10.1063/1.126300

Erdemir, A., and Donnet, C. (2006). Tribology of diamond-like carbon films: recent progress and future prospects. *J. Phys. D Appl. Phys.* 39, R311–R327. doi:10.1088/0022-3727/39/18/r01

Fan, X., Wei, G., Lin, X., Wang, X., Si, Z., Zhang, X., et al. (2020). Reversible switching of interlayer exchange coupling through atomically thin VO2 via electronic state modulation. *Matter* 2, 1582–1593. doi:10.1016/j.matt.2020.04.001

Ghadai, R. K., Das, S., Kumar, D., Mondal, S. C., and Swain, B. P. (2018). Correlation between structural and mechanical properties of silicon doped DLC thin films. *Diam. Relat. Mat.* 82, 25–32. doi:10.1016/j.diamond.2017.12.012

Ghadai, R. K., Singh, K., Sharma, A., Roy, M. K., and Swain, B. P. (2021). Mechanical and Tribological properties of metal incorporated DLC thin film. *Nanostructured Mater. their Appl.*, 229–263. doi:10.1007/978-981-15-8307-0_12

Guo, T., Kong, C., Li, X., Guo, P., Wang, Z., and Wang, A. (2017). Microstructure and mechanical properties of Ti/Al co-doped DLC films: dependence on sputtering current, source gas, and substrate bias. *Appl. Surf. Sci.* 410, 51–59. doi:10.1016/j.apsusc.2017.02.254

Han, C. X., Zhi, J. Q., Zeng, Z., Wang, Y. S., Zhou, B., Gao, J., et al. (2023). Synthesis and characterization of nano-polycrystal diamonds on refractory high entropy alloys by chemical vapour deposition. *Appl. Surf. Sci.* 623, 157108. doi:10.1016/j.apsusc.2023.157108

He, H. T., Fang, J. X., Wang, J. X., Sun, T., Yang, Z., Ma, B., et al. (2023). Carbide-reinforced Re0.1Hf0.25NbTaW0.4 refractory high-entropy alloy with excellent room and elevated temperature mechanical properties. *Int. J. Refract. Hard Mater.* 116, 106349. doi:10.1016/j.ijrmhm.2023.106349

He, Y., Wang, F., Du, G., Pan, L., Wang, K., Gerhard, R., et al. (2022). Revisiting the thermal ageing on the metallised polypropylene film capacitor: from device to dielectric film. *High. Volt.* 8, 305–314. doi:10.1049/hve2.12278

Huang, J., Peng, J., Qiu, X., and Li, X. (2023a). Evolution of the microstructure, hybridization, and internal stress of Al-doped Diamond-like carbon coatings: a molecular dynamics simulation. *Langmuir* 39, 3895–3904. doi:10.1021/acs.langmuir.2c03200

Huang, J., Peng, J., Qiu, X., and Li, X. (2023b). Evolution of the microstructure, hybridization, and internal stress of Al-doped diamond-like carbon coatings: a molecular dynamics simulation. *Langmuir* 39, 3895–3904. doi:10.1021/acs.langmuir.2c03200

Irudayaraj, A. A., Kuppusami, P., Thirumurugesan, R., Mohandas, E., Kalainathan, S., and Raghunathan, V. S. (2007). Influence of nitrogen flow rate on growth of TiAlN films prepared by DC magnetron sputtering. *Surf. Eng.* 23, 7–11. doi:10.1179/174329407x161627

Kong, C., Guo, P., Sun, L., Zhou, Y., Liang, Y., Li, X., et al. (2018). Tribological mechanism of diamond-like carbon films induced by Ti/Al co-doping. *Surf. Coatings Technol.* 342, 167–177. doi:10.1016/j.surfcoat.2018.02.098

Kong, D., and Fu, G. (2015). Nanoindentation analysis of TiN, TiAlN, and TiAlSiN coatings prepared by cathode ion plating. *Sci. China Technol. Sci.* 58, 1360–1368. doi:10.1007/s11431-015-5876-2

Lai, L., Gan, M., Wang, J., Chen, L., Liang, X., Feng, J., et al. (2023). New class of high-entropy rare-earth niobates with high thermal expansion and oxygen insulation. *J. Am. Ceram. Soc.* 106, 4343–4357. doi:10.1111/jace.19077

Liang, J. H., Chen, M. H., Tsai, W. F., Lee, S. C., and Ai, C. F. (2007). Characteristics of diamond-like carbon film synthesized on AISI 304 austenite stainless steel using plasma immersion ion implantation and deposition. *Nucl. Instrum. Methods Phys. Res. B* 257, 696–701. doi:10.1016/j.nimb.2007.01.143

Liu, E., Li, L., Blanpain, B., and Celis, J. P. (2005). Residual stresses of diamond and diamondlike carbon films. *J. Appl. Phys.* 98, 073515. doi:10.1063/1.2071451

Matei, A. A., Pencea, I., Branzei, M., Trancă, D. E., Ţepeş, G., Sfăt, C. E., et al. (2015). Corrosion resistance appraisal of TiN, TiCN and TiAlN coatings deposited by CAE-PVD method on WC–Co cutting tools exposed to artificial sea water. *Appl. Surf. Sci.* 358, 572–578. doi:10.1016/j.apsusc.2015.08.041

Ni, W., Cheng, Y.-T., Weiner, A. M., and Perry, T. A. (2006). Tribological behavior of diamond-like-carbon (DLC) coatings against aluminum alloys at elevated temperatures. *Surf. Coatings Technol.* 201, 3229–3234. doi:10.1016/j.surfcoat.2006.06.045

Pang, H., Wang, X., Zhang, G., Chen, H., Lv, G., and Yang, S. (2010). Characterization of diamond-like carbon films by SEM, XRD and Raman spectroscopy. *Appl. Surf. Sci.* 256 (21), 6403–6407. doi:10.1016/j.apsusc.2010.04.025

Patel, N. G., Sreeram, A., Venkatanarayanan, R. I., Krishnan, S., and Yuya, P. A. (2015). Elevated temperature nanoindentation characterization of poly(para-phenylene vinylene) conjugated polymer films. *Polym. Test.* 41, 17–25. doi:10.1016/j.polymertesting.2014.10.004

Peng, X. L., and Clyne, T. W. (1998). Residual stress and debonding of DLC films on metallic substrates. *Diam. Relat. Mat.* 7, 944–950. doi:10.1016/s0925-9635(97)00331-2

Pu, J., Zhang, G., Wan, S., and Zhang, R. (2015). Synthesis and characterization of low-friction Al-DLC films with high hardness and low stress. *J. Compos. Mat.* 49, 199–207. doi:10.1177/0021998313515291

Robertson, J. (2002). Diamond-like amorphous carbon. *Mat. Sci. Eng. R. Rep.* 37, 129–281. doi:10.1016/s0927-796x(02)00005-0

Singh, V., Jiang, J. C., and Meletis, E. I. (2005). Cr-diamondlike carbon nanocomposite films: synthesis, characterization and properties. *Thin Solid Films* 489, 150–158. doi:10.1016/j.tsf.2005.04.104

Tay, B. K., Cheng, Y. H., Ding, X. Z., Lau, S. P., Shi, X., You, G. F., et al. (2001). Hard carbon nanocomposite films with low stress. *Diam. Relat. Mat.* 10, 1082–1087. doi:10.1016/s0925-9635(00)00429-5

Voevodin, A. A., O'neill, J. P., and Zabinski, J. S. (1999). Nanocomposite tribological coatings for aerospace applications. *Surf. Coatings Technol.* 116, 36–45. doi:10.1016/s0257-8972(99)00228-5

Wang, J., Chong, X., Lv, L., Wang, Y., Ji, X., Yun, H., et al. (2023). High-entropy ferroelastic (10RE0.1)TaO4 ceramics with oxygen vacancies and improved thermophysical properties. *J. Mat. Sci. Technol.* 157, 98–106. doi:10.1016/j.jmst.2022.12.027

Wang, J., Pan, Z., Wang, Y., Wang, L., Su, L., Cuiuri, D., et al. (2020). Evolution of crystallographic orientation, precipitation, phase transformation and mechanical properties realized by enhancing deposition current for dual-wire arc additive manufactured Ni-rich NiTi alloy. *Addit. Manuf.* 34, 101240. doi:10.1016/j.addma.2020.101240

Wongpanya, P., Silawong, P., and Photongkam, P. (2022). Adhesion and corrosion of Al–N doped diamond-like carbon films synthesized by filtered cathodic vacuum arc deposition. *Ceram. Int.* 48, 20743–20759. doi:10.1016/j.ceramint.2022.04.055

Xie, J., Chen, Y., Yin, L., Zhang, T., Wang, S., and Wang, L. (2021). Microstructure and mechanical properties of ultrasonic spot welding TiNi/Ti6Al4V dissimilar materials using pure Al coating. *J. Manuf. Process.* 64, 473–480. doi:10.1016/j.jmapro.2021.02.009

Yang, Y. (2016). Sensitivity of nanoindentation strain rate in poly(ester-ester-ketone) using atomic force microscopy. *Polym. Test.* 53, 85–88. doi:10.1016/j.polymertesting.2016.05.013

Zhang, J., Wang, L., Zhong, A., Huang, G., Wu, F., Li, D., et al. (2019). Deep red PhOLED from dimeric salophen Platinum(II) complexes. *Dyes Pigm* 162, 590–598. doi:10.1016/j.dyepig.2018.10.053

Zhang, P., Tay, B. K., Sun, C. Q., and Lau, S. P. (2002). Microstructure and mechanical properties of nanocomposite amorphous carbon films. *J. Vac. Sci. Technol. A* 20, 1390–1394. doi:10.1116/1.1486227

Zhou, Y., Guo, P., Sun, L., Liu, L., Xu, X., Li, W., et al. (2019). Microstructure and property evolution of diamond-like carbon films co-doped by Al and Ti with different ratios. *Surf. Coat. Technol.* 361, 83–90. doi:10.1016/j.surfcoat.2019.01.049